



Published in final edited form as:

Clin Immunol. 2015 January ; 156(1): 1–8. doi:10.1016/j.clim.2014.10.004.

A chimeric human–mouse model of Sjögren's syndrome

Nicholas A. Young^{a,b,d}, Lai-Chu Wu^{a,b,d}, Michael Bruss^{a,b,d}, Benjamin H. Kaffenberger^{a,b,d}, Jeffrey Hampton^{a,b,d}, Brad Bolon^{c,d}, and Wael N. Jarjour^{a,b,d,*}

^aDivision of Rheumatology and Immunology, The Ohio State University, Columbus, OH 43210, USA

^bDepartment of Internal Medicine, The Ohio State University, Columbus, OH 43210, USA

^cDepartment of Veterinary Biosciences and the Comparative Pathology and Mouse Phenotyping Shared Resource, The Ohio State University, Columbus, OH 43210, USA

^dWexner Medical Center at The Ohio State University, Columbus, OH 43210, USA

Abstract

Despite recent advances in the understanding of Sjögren's Syndrome (SjS), the pathogenic mechanisms remain elusive and an ideal model for early drug discovery is not yet available. To establish a humanized mouse model of SjS, peripheral blood mononuclear cells (PBMCs) from healthy volunteers or patients with SjS were transferred into immunodeficient NOD-scid IL-2 γ (null) mouse recipients to produce chimeric mice. While no difference was observed in the distribution of cells, chimeric mice transferred with PBMCs from SjS patients produced enhanced cytokine levels, most significantly IFN- γ and IL-10. Histological examination revealed enhanced inflammatory responses in the lacrimal and salivary glands of SjS chimeras, as measured by digital image analysis and blinded histopathological scoring. Infiltrates were primarily CD4⁺, with minimal detection of CD8⁺ T-cells and B-cells. These results demonstrate a novel chimeric mouse model of human SjS that provides a unique *in vivo* environment to test experimental therapeutics and investigate T-cell disease pathology.

Keywords

Sjögren's syndrome; Chimera; Animal model; Humanized mouse

1. Introduction

Sjögren's syndrome (SjS) is one of the most prevalent autoimmune diseases, with affects ranging between 0.5 and 3% of a given population. Although systemic inflammatory responses are observed, this autoimmune disease mainly affects the salivary and lacrimal glands. Glandular histopathology is primarily characterized by a CD4⁺ T-cell infiltrate [1]. Despite the detection of B-cells in advanced lesions [2], T-cells predominate the infiltrate

This is an open access article under the CC BY-NC-ND license (<http://creativecommons.org/licenses/by-nc-nd/3.0/>).

*Corresponding author at: Rm S2056 Davis Medical Research Center, 480 Medical Center Dr, Columbus, OH 43210, USA. Fax: +1 614 293 5361. Wael.Jarjour@osumc.edu (W.N. Jarjour).

Conflict of interest and Financial disclosure: There were no conflicts of interest to report in this study.

and appear to mediate the cytotoxic pathology and inflammatory cytokine biology associated with SjS (reviewed in [3]). While the trigger of the cellular infiltration remains unknown, the pathogenesis of SjS is currently thought to involve genetic, neuro-hormonal and environmental factors, and to require participation of the innate and the adaptive immune systems. Thus, research concerning SjS development, progression, and molecular-based therapeutics requires *in vivo* animal models.

Aside from type 1 diabetes, NSG mice have not been used extensively in the investigation of autoimmune disorders. Here, we take advantage of the NSG model to engraft and study SjS. The resulting SjS chimeras displayed enhanced cytokine expression and target organ inflammation relative to transfers from healthy controls. Further, histopathological analysis revealed marked inflammation and tissue damage in the salivary and lacrimal glands consisting primarily of CD4⁺ T-cell infiltrates. Collectively, this approach has provided a novel platform to explore human-focused, molecular-based therapies for targeting T-cells in SjS and more readily enables the future translational application of these findings.

2. Materials and methods

2.1. Human samples and PBMC isolation

Patients meeting the revised American–European consensus criteria for SjS ($n = 4$) [7] as well as age and sex-matched healthy volunteers ($n = 4$) were recruited for the study from The Ohio State University Wexner Medical Center (OSUWMC) clinics, the Research Match program at OSUWMC, and the American Red Cross. Participation was through an approved Institutional Review Board protocol. PBMCs were isolated under Ficoll gradient centrifugation as previously described [8].

2.2. Mice

4-week old NOD.Cg-Prkdcscid Il2rgtm1Wjl/SzJ (NSG) mice were obtained from The Jackson Laboratories. All animal maintenance and protocols are approved by the Institutional Animal Care and Use Committee at OSUWMC. Animal facility was maintained at 22–23 °C and between 30 and 50% relative humidity with a 12-hour light/dark cycle. Chow and water were available *ad libitum*.

2.3. Adoptive transfers

Freshly isolated human PBMCs were injected intraperitoneally into 8-week old NSG mice (5.0×10^6 cells/mouse); at least 3 mice were injected from each individual human sample. Human PBMC preparations were washed in PBS and counted using a hemocytometer with trypan blue to ensure cell viability. All samples were kept separate and not pooled before injections. Mice ($n = 14$ total for each experimental condition; healthy or SjS) were monitored every other day, including weights and physical signs of disease progression, and sacrificed 4 weeks after adoptive transfer for blood and tissue collection as described below.

2.4. Tissue collection and staining

Mouse tissues were dissected, submerged in neutral buffered 10% formalin, and transferred to 70% ethanol for paraffin processing. Paraffin blocks were cut at 4 microns, placed on positively charged slides, and fixed in cold acetone. Serial paraffin sections were used for immunohistochemistry and hematoxylin and eosin (H&E) staining as previously described [9]. Briefly, all slides were stained in Richard Allan Scientific Hematoxylin (Thermo Scientific, Waltham, MA) and Eosin-Y (Thermo Scientific) with the Leica Autostainer (Leica Biosystems, Buffalo Grove, IL). Immunohistochemistry was performed with antibodies for CD4 (Leica Biosystems), CD8 (Dako, Carpinteria, CA) CD20 (Dako), and CD68 (Dako) using the Dako Autostainer system according to manufacturer's protocol.

2.5. Image analysis and histopathology scoring

Slides were scanned using the Aperio ScanScope XT eSlide capture device (Aperio, Vista, CA), and analyzed by Aperio ImageScope digital analysis software (v9.1) as detailed formerly to quantitate inflammation by H&E and to determine lymphocyte localization by immunohistochemistry [9].

H&E-stained paraffin sections of lacrimal and salivary glands were subjected to blinded histopathological analysis by a board-certified veterinary pathologist (BB) as described previously [9]. Inflammation and acinar epithelial necrosis were scored 0–4: 0, no epithelial degeneration or necrosis and no inflammatory cells observed in the connective tissue between acini (inflammation within normal limits); 1, minimal inflammation observed with few inflammatory cells present in the connective tissue between acini and occasional cytoplasmic vacuolation of acinar epithelial cells; 2, mild inflammation characterized by scattered, small clusters of cells in the connective tissue and between acini with nuclear fragmentation of some acinar epithelial cells; 3, moderate inflammation consisting of substantial inflammatory cell presence with larger, coalescing clusters in the connective tissue with a widespread reduction in acinar and duct size; 4, marked inflammation defined by inflammatory cells covering most of the organ and an essential absence of the acinar epithelium.

2.6. Flow cytometry

Blood was collected from chimeric mice by submandibular bleeding and leukocytes were purified for flow cytometry using red blood cell lysis solution (eBioscience, San Diego, CA) following the manufacturer's protocol. Cells were labeled with antibodies for anti-human CD3 (eBioscience), CD4 (Immunotech, Vaudreuil-Dorion, Canada), CD8 (Caltag Laboratories, Buckingham, United Kingdom), CD20 (eBioscience), CD14 (eBioscience), or CD56 (eBioscience) following the manufacturer's protocol. Data was collected on the BD FACS Calibur platform (BD Biosciences, San Jose, CA) using CellQuest Pro (v5.1, BD Biosciences) and exported for analysis via FlowJo (v.7.6.5, Tree Star, Inc, Ashland, OR).

2.7. Cytokine ELISA

Cytokine analysis was performed on serum collected from chimeric mice at the time of sacrifice using a cocktail of Bio-Plex Pro® single-plex magnetic beads (Bio-Rad, Hercules, CA) on the Bio-Plex 200 system according to the manufacturer's protocol. Data analysis was

performed using Bio-Plex Manager® (v5.0) software and results were exported to Microsoft Excel (v2010) for further analysis.

2.8. Salivary gland function

Salivary gland function was tested following pilocarpine stimulation (1 µg/g body weight) according to previously described methods [10]. Briefly, mice were restrained, injected with pilocarpine intraperitoneally, and observed until the appearance of saliva, which was collected for 5 min and pooled as a measurement of salivary gland function. Weights of collection tubes were measured individually before and after saliva collection and the differences were recorded for analysis.

2.9. Statistics

All numerical data were expressed as mean values ± standard deviation. Statistical differences were determined by paired, two-tailed, Student *t* tests using Microsoft Excel (v2010) and considered statistically significant if $p < 0.05$.

3. Results

3.1. Humanized SjS mouse blood contains donor T cells and has enhanced cytokine levels

To establish a novel chimeric mouse model of SjS, immuno-deficient NSG mice were adoptively transferred with 5×10^6 PBMCs isolated from healthy volunteers and patients diagnosed with primary SjS [7]. At the time of transfer, all human PBMC populations expressed similar and detectable levels of markers for T-cells (CD3, CD4, and CD8), B-cells (CD20), Natural killer cells (NK; CD56), and macrophages (CD68), as determined by flow cytometry (data not shown). Four weeks later, whole blood was collected from humanized mice; our results show that CD4⁺ and CD8⁺ T-cells were the only detectable human leukocyte subsets in both healthy and SjS chimeras (Fig. 1A). Also, no significant differences were observed in the cell numbers for CD3⁺, CD4⁺, and CD8⁺ T-cell distribution between mice receiving SjS or healthy PBMCs (Fig. 1B). Despite positive detection in serum from SjS patients, anti-nuclear antibodies were not detected at 4 weeks in any chimeric mouse (unpublished observation).

To further examine potential differences between these humanized mice, serum from healthy and SjS chimeras was collected at 28 days to compare human cytokine levels by ELISA. SjS chimeras expressed increased IFN-γ by 2.4-fold ($p < 0.05$), IL-10 by 2.7-fold ($p < 0.05$), IL-17 by 6-fold, IL-2 by 3-fold, IL-6 by 74-fold, and TNF-α by 21-fold compared to the serum levels of cytokines in the chimeric control mice (Fig. 1C). While levels of IL-4 (0.1 pg/mL) and IFN-α (8.4 pg/mL) were measured in SjS chimeric mice, they were undetectable following transfer of healthy human PBMCs (Fig. 1C). MIP-1β expression was detected in all mice, but no difference was observed (Fig. 1C).

3.2. SjS chimeras display increased target organ inflammation and disease pathology

To determine the extent of inflammation in the lacrimal and salivary glands, chimeric mouse tissue was stained with H&E for histopathological scoring and digital image analysis. The initial histological assessment indicated that the lacrimal and salivary glands of SjS chimeras

had markedly more inflammation when compared to healthy PBMC adoptive transfers (Fig. 2A). Sialoadenitis that was induced by the transfer of human SjS PBMCs consisted primarily of lymphocytes, which led to destruction of acinar epithelium with increasing inflammation. In the submandibular salivary gland, enhanced inflammation typically was accompanied by reduced prominence of ducts, increased distance between ducts due to infiltration of inflammatory cells into the connective tissue, and acinar loss. Dacryoadenitis in the SjS chimeras also displayed enhanced lymphocytic infiltrates and acinar epithelial destruction when compared to the lacrimal glands of mice transferred with PBMCs from healthy controls, which had little to no inflammation present (Fig. 2A). In concordance, digital image analysis to quantitate the extent of inflammation in the target organs resulted in statistically significant values that were 2-fold higher in both the salivary and lacrimal glands of SjS chimeras (Fig. 2B). Blinded, semi-quantitative histopathological scoring of H&E stains offered further confirmation of this conclusion; healthy human PBMC transfers scored within normal limits (0–1) for the salivary and lacrimal gland, while those transferred from SjS patients scored 2.6 ± 0.5 ($p < 0.05$) and 3.25 ± 0.5 ($p < 0.05$), respectively (Fig. 2C).

To demonstrate the effects and specificity of target organ inflammation, salivary gland function was measured and additional tissue sections were analyzed in the chimeric mice. Saliva was collected from healthy and SjS chimeras following pilocarpine stimulation to examine loss of end-organ function. While no difference in salivary gland function was observed 0, 1, or 2 weeks following adoptive transfer, saliva production was significantly reduced 36% ($p < 0.05$) by SjS cells 4 weeks post-transfer (Fig. 2D). H&E stained tissue sections of the skin, intestine, kidney, and liver did not reveal any substantial inflammatory responses and no histopathological differences were observed between SjS and healthy transfers (Fig. 2E).

3.3. Lymphocytic infiltrates of target organs are predominately CD4⁺ T cells

Histopathology of salivary and lacrimal glands from SjS patients is comprised mostly of CD4⁺ T-cells with CD8⁺ T-cells and B-cells detected to a lesser extent, which suggests that T-cells are the primary effector cells of target organ inflammation and glandular dysfunction [11,12]. To characterize the salivary and lacrimal gland infiltrates of our chimeric mice, immunohistochemistry was performed to detect T-cells (CD4 and CD8), B-cells (CD20), NK cells (CD56), and macro phages (CD68). Subsequently, the slides were scanned for digital imaging and quantitative comparison by measuring the pixel intensity of positive staining. Immunohistochemical analysis of the salivary glands from SjS chimeras revealed an enhancement of 2.7-fold ($p < 0.0001$) in CD4⁺ T-cells, 6.7-fold ($p < 0.0001$) in CD8⁺ T-cells, and 4.1-fold ($p < 0.0001$) in B-cells when compared to PBMC transfers from healthy controls (Fig. 3A). Further, positive staining of CD4⁺ T-cells in SjS chimeras was greater by 4.4-fold ($p < 0.0001$) and 18.5-fold ($p < 0.0001$) when compared to that of CD8⁺ T-cells and B-cells, respectively (Fig. 3A). Similarly, image analyses of lacrimal gland infiltrates from SjS chimeras were significantly greater than the control counterparts by 4.0-fold ($p < 0.0001$) for CD4⁺ T-cells, 7.0-fold ($p < 0.0001$) for CD8⁺ T-cells, and 9.1-fold ($p < 0.0001$) for B-cells (Fig. 3B). Levels of CD4⁺ T-cells in the lacrimal glands of the SjS chimeras were also significantly higher than CD8⁺ T-cells (3.3-fold; $p < 0.0001$) and B-cells (15-fold; $p <$

0.0001) (Fig. 3B). Staining for macrophages and NK cells revealed no significant detection in either the lacrimal or salivary glands of all adoptively transferred chimeric mice (Fig. 3A-B). These data demonstrate that the histological patterns of target organ inflammation in this chimeric mouse model of SjS are largely within the pathological spectrum of what is observed in SjS patients with notable exceptions [13].

4. Discussion

In order for novel therapies targeting specific immune cell function to move forward in human clinical trials, it is critical to examine the potential efficacy/side effects in established preclinical animal models. However, an animal model of SjS that is suitable for early drug discovery is not yet available. In this work, we have developed a novel SjS chimeric model to replicate T-cell mediated autoimmune pathology *in vivo*. This humanized mouse model could be an appropriate platform to be used in the discovery of therapeutic alternatives to the current management of SjS, which is non-specific and largely supportive.

Since graft *versus* host inflammation is not observed in the NSG mouse strain for at least 30 days following adoptive transfer [5], we exploited this 4-week timeframe to explore human SjS autoimmune responses in our mouse chimeras. The transfer of PBMCs from SjS patients results in robust CD4⁺ T-cell infiltration in the salivary and lacrimal glands at 28 days when compared to transfers from healthy subjects. Notably, chimeric mice receiving healthy PBMCs did have detectable levels of infiltrate in the salivary and lacrimal glands at 28 days. This may be attributable to the propensity of NOD mice to develop sialoadenitis and that this autoimmune phenotype is transferrable to NOD-scid mice [6], which indicates that an environment permissive to an inflammatory response is presumably present to some extent already in the NSG mice.

While the circulating T-cell distribution was similar in all chimeric mice in this study, mice transferred with PBMCs from SjS patients produced significantly higher levels of IFN- γ , IL-6, IL-10, IL-17, and TNF- α . Accordingly, both IFN- γ and IL-10 were found to be elevated in peripheral blood T-cells of SjS patients [14]. IFN- γ and TNF- α are major cytokines involved in the promotion of Th₁ pro-inflammatory responses and have been shown to be elevated in the saliva of SjS patients [15]. Moreover, mouse models of SjS have shown that IFN- γ deficiency prevents clinical onset and tissue-specific autoimmune responses [16]. Despite the traditional role as a Th₂ anti-inflammatory cytokine, IL-10 levels are elevated in the serum [17] of SjS patients and correlate with disease activity, thus suggesting a potentially pathogenic role for IL-10 in the presence of IFN- γ [18]. In addition, IL-6 and IL-17 are cytokines involved in the Th₁₇ pathway and have been implicated in multiple autoimmune diseases, including SjS. Considering the recent success using monoclonal antibodies to neutralize inflammatory mediators in the treatment of other autoimmune disorders, our results suggest targeting of IFN- γ , IL-17, and IL-10 as a viable therapeutic strategy to treat SjS. Furthermore, since some degree of activation of Th₁, Th₂, and Th₁₇ pathways is observed both in this model and in human SjS, these chimeras may provide an ideal study medium to examine the differential blockade of each of these pathways on the final disease state to determine the pathological role of each.

Our histopathological and immunohistochemical findings recapitulate what is seen with regard to T-cells in SjS patients, which renders this model useful for the study of molecular-based therapies to treat and prevent disease pathology. Additionally, because immunohistochemical data on lacrimal glands in SjS is lacking due to the inaccessibility of this tissue in humans for biopsy, our model provides a mechanism to analyze this tissue. Our data indicate that the extent and pattern of inflammation in the lacrimal gland are indeed similar to the salivary gland in SjS. Histopathological scores of SjS chimeras were defined by enhanced lymphocytic infiltrates and acinar epithelial necrosis, leading to a widespread reduction in duct size. Digital imaging of immunohistochemistry showed that salivary and lacrimal gland infiltrates were predominately CD4⁺ T-cells, with minimal levels of CD8⁺ T-cells and B-cells. In concordance, previous work has demonstrated that CD4⁺ T-cells predominate the salivary gland infiltrate of SjS patients [1] and that these cells are largely responsible for mediating glandular destruction [3]. Consistent with previously published studies demonstrating possible roles for other immune cells in SjS, B-cells were present at significantly greater levels in lacrimal and salivary gland infiltrates when compared to transfers from healthy donors [2].

5. Conclusion

Collectively, adoptive transfer of PBMCs from SjS patients into NSG mice should be a novel chimeric mouse model of SjS that will allow the *in vivo* study of autoimmune-mediated inflammation on human immune cells and opens new avenues to study disease progression and therapeutic intervention. Although, considering the heterogeneity of SjS and that the disease transferred in this model will be patient-specific, therapeutic efficacy would have to be demonstrated in adoptive transfers from a number of patients before reaching definitive conclusions. Further examination using this SjS model will be in characterizing the *in situ* glandular histopathology of SjS chimeras. Subsequently, this model will be used to examine gene expression and characterize the effector T-cell population to facilitate the investigation of molecular-based therapies to prevent target organ inflammation in SjS and other autoimmune disorders.

Acknowledgments

We would like to acknowledge all the volunteers that participated in this study, the American Red Cross for assistance in sample acquisition, and Research Match at OSUWMC. We would also like to thank Alan Flechtner of the Comparative Pathology and Mouse Phenotyping Shared Resource at OSUWMC and Kristin Kovach of OSUWMC for their work in preparing and staining tissue samples.

Funding for this work was provided through The Ohio State University's Wexner Medical Center and the Richmond Eye and Ear Foundation. The Center for Clinical and Translational Science's Research Match program is funded through CTSA grant number UL1TR000090. The Comparative Pathology and Mouse Phenotyping Shared Resource is supported in part by grant P30 CA016058, National Cancer Institute.

References

1. Ramos-Casals M, Font J. Primary Sjogren's syndrome: current and emergent aetiopathogenic concepts. *Rheumatology*. 2005; 44:1354–1367. [PubMed: 15956090]
2. Christodoulou MI, Kapsogeorgou EK, Moutsopoulos HM. Characteristics of the minor salivary gland infiltrates in Sjogren's syndrome. *J Autoimmun*. 2010; 34:400–407. [PubMed: 19889514]

3. Singh N, Cohen PL. The T cell in Sjogren's syndrome: force majeure, not spectateur. *J Autoimmun.* 2012; 39:229–233. [PubMed: 22709856]
4. Shultz LD, Ishikawa F, Greiner DL. Humanized mice in translational biomedical research. *Nat Rev Immunol.* 2007; 7:118–130. [PubMed: 17259968]
5. King M, Pearson T, Shultz LD, Leif J, Bottino R, Trucco M, et al. A new Hu-PBL model for the study of human islet alloreactivity based on NOD-scid mice bearing a targeted mutation in the IL-2 receptor gamma chain gene. *Clin Immunol.* 2008; 126:303–314. [PubMed: 18096436]
6. Christianson SW, Shultz LD, Leiter EH. Adoptive transfer of diabetes into immunodeficient NOD-scid/scid mice. Relative contributions of CD4+ and CD8+ T-cells from diabetic versus prediabetic NOD.NON-Thy-1a donors. *Diabetes.* 1993; 42:44–55. [PubMed: 8093606]
7. Vitali C, Bombardieri S, Jonsson R, Moutsopoulos HM, Alexander EL, Carsons SE, et al. Classification criteria for Sjogren's syndrome: a revised version of the European criteria proposed by the American–European Consensus Group. *Ann Rheum Dis.* 2002; 61:554–558. [PubMed: 12006334]
8. Young NA, Friedman AK, Kaffenberger B, Rajaram MV, Birmingham DJ, Rovin BH, et al. Novel estrogen target gene ZAS3 is overexpressed in systemic lupus erythematosus. *Mol Immunol.* 2013; 54:23–31. [PubMed: 23178823]
9. Young NA, Sharma R, Friedman AK, Kaffenberger BH, Bolon B, Jarjour WN. Aberrant muscle antigen exposure is sufficient to cause myositis in a regulatory T cell–deficient milieu. *Arthritis Rheum.* 2013; 65:3259–3270. [PubMed: 24022275]
10. Sharma R, Zheng L, Guo X, Fu SM, Ju ST, Jarjour WN. Novel animal models for Sjogren's syndrome: expression and transfer of salivary gland dysfunction from regulatory T cell-deficient mice. *J Autoimmun.* 2006; 27:289–296. [PubMed: 17207605]
11. Adamson TC III, Fox RI, Frisman DM, Howell FV. Immunohistologic analysis of lymphoid infiltrates in primary Sjogren's syndrome using monoclonal antibodies. *J Immunol.* 1983; 130:203–208. [PubMed: 6600176]
12. Pepose JS, Akata RF, Pflugfelder SC, Voigt W. Mononuclear cell phenotypes and immunoglobulin gene rearrangements in lacrimal gland biopsies from patients with Sjogren's syndrome. *Ophthalmology.* 1990; 97:1599–1605. [PubMed: 1965021]
13. Rusakiewicz S, Nocturne G, Lazure T, Semeraro M, Flament C, Caillat-Zucman S, et al. NCR3/NKp30 contributes to pathogenesis in primary Sjogren's syndrome. *Sci Transl Med.* 2013; 5:195ra96.
14. Villarreal GM, Alcocer-Varela J, Llorente L. Cytokine gene and CD25 antigen expression by peripheral blood T cells from patients with primary Sjogren's syndrome. *Autoimmunity.* 1995; 20:223–229. [PubMed: 7578884]
15. Kang EH, Lee YJ, Hyon JY, Yun PY, Song YW. Salivary cytokine profiles in primary Sjogren's syndrome differ from those in non-Sjogren sicca in terms of TNF-alpha levels and Th-1/Th-2 ratios. *Clin Exp Rheumatol.* 2011; 29:970–976. [PubMed: 22132900]
16. Cha S, Brayer J, Gao J, Brown V, Killedar S, Yasunari U, et al. A dual role for interferon-gamma in the pathogenesis of Sjogren's syndrome-like autoimmune exocrinopathy in the nonobese diabetic mouse. *Scand J Immunol.* 2004; 60:552–565. [PubMed: 15584966]
17. Perrier S, Serre AF, Dubost JJ, Beaujon G, Plazonnet MP, Albuissou E, et al. Increased serum levels of interleukin 10 in Sjogren's syndrome; correlation with increased IgG1. *J Rheumatol.* 2000; 27:935–939. [PubMed: 10782819]
18. Sharif MN, Tassioulas I, Hu Y, Mecklenbrauker I, Tarakhovsky A, Ivashkiv LB. IFN-alpha priming results in a gain of proinflammatory function by IL-10: implications for systemic lupus erythematosus pathogenesis. *J Immunol.* 2004; 172:6476–6481. [PubMed: 15128840]

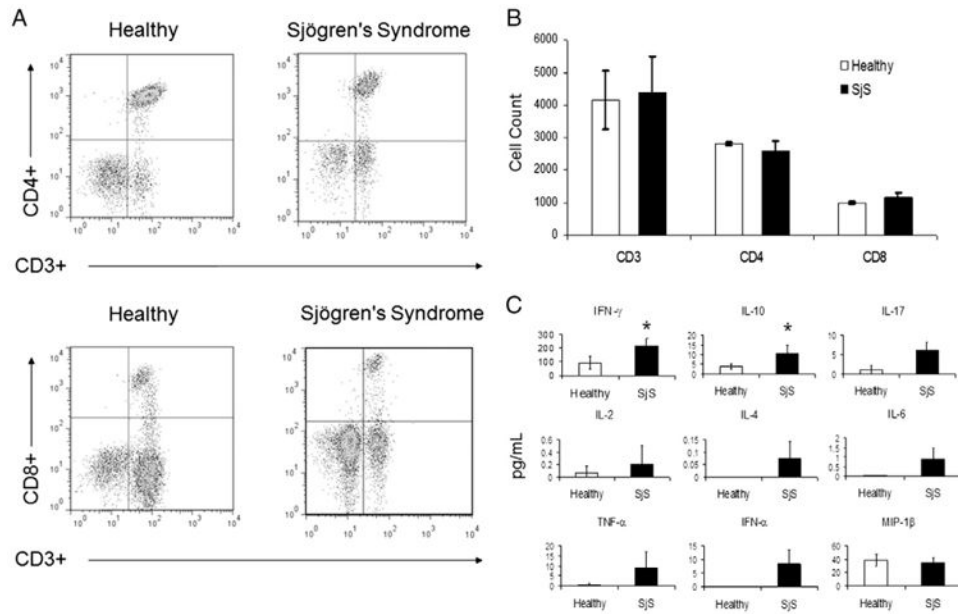


Figure 1.

The predominately T-cell-mediated recovery following engraftment of PBMCs from patients with Sjögren's syndrome (SjS) is similar to healthy controls, but produces enhanced cytokine levels. PBMCs were isolated from whole blood samples obtained from SjS patients ($n = 4$) or healthy controls ($n = 4$) and adoptively transferred intraperitoneally into NOD *scid* gamma (NSG) mice (at least 3 mice injected per sample) for 28 days. (A) Analysis of mouse whole blood for CD3⁺/CD4⁺ or CD3⁺/CD8⁺ T-cells by flow cytometry. (B) Cell counts for CD3⁺, CD4⁺, and CD8⁺ T-cells. (C) Analysis of serum cytokines by ELISA. Values are the mean \pm SD ($n = 6$). * = $P < 0.05$ versus healthy.

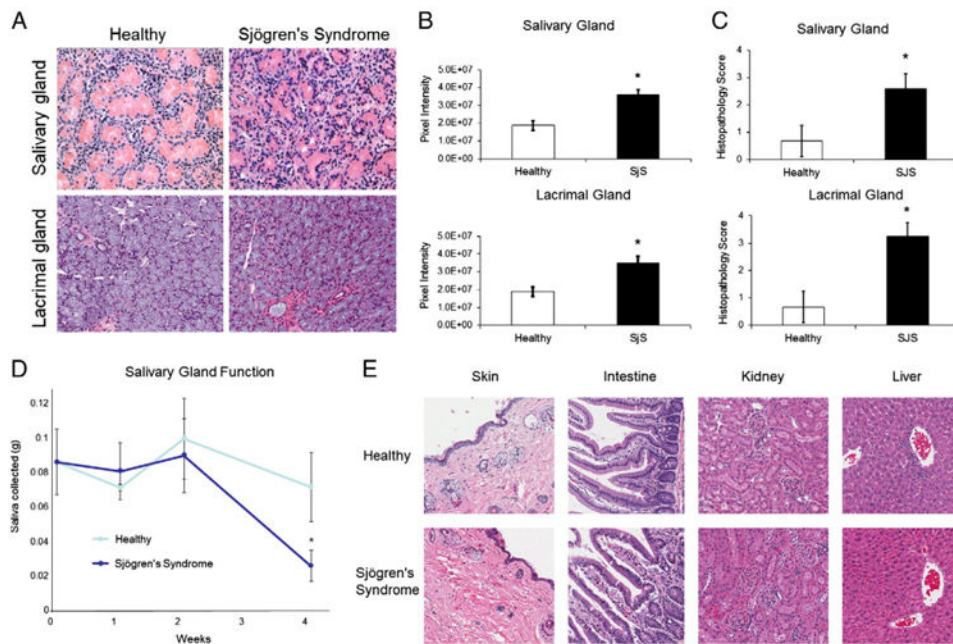


Figure 2.

Adoptive transfer of PBMCs from Sjögren's syndrome (SjS) patients into immunodeficient mice results in enhanced target organ inflammation and reduced salivary gland function. Salivary gland and lacrimal gland tissues were harvested from chimeric mice 28 days after adoptive transfer with PBMC preparations from healthy controls or SjS patients. (A) Hematoxylin and eosin (H&E) stains of paraffin-embedded mouse tissue sections. (B) Extent of inflammation induced by adoptive transfer of healthy or SjS cells, as assessed quantitatively by digital image analysis of H&E slides. (C) Histopathologic scores of the H&E-stained tissue sections, as determined by blinded semi-quantitative histopathologic analysis. (D) Salivary gland function was measured by saliva production in mice following pilocarpine stimulation via intraperitoneal injection (1 $\mu\text{g/g}$ body weight). (E) H&E stained tissue sections of NSG mice at 28 days. Original magnification $\times 200$. Values are the mean \pm SD ($n = 6$). * = $P < 0.05$ versus healthy.

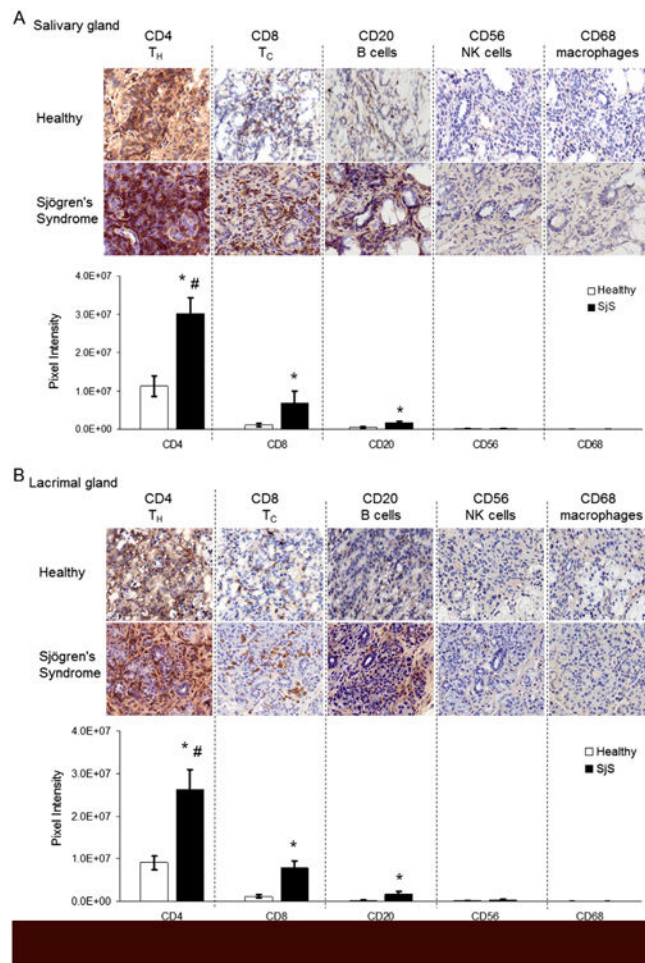


Figure 3.

Target organ inflammatory responses in chimeric mice engrafted with PBMCs from Sjögren's syndrome (SjS) patients consist chiefly of CD4⁺ T-cells. Salivary and lacrimal gland tissue sections from NSG mice were immunohistochemically stained for human CD4, CD8, CD20, CD56, and CD68 expression 28 days after adoptive transfer. (A) and (B) Inflammatory cell surface marker expression within infiltrates of salivary glands (A) or lacrimal glands (B), as determined by immunohistochemistry (top) and digital image analysis (bottom). Values are the mean \pm SD and results are representative of trends observed in at least 4 mice ($n = 2$ independent experiments) from each PBMC source (healthy or SjS). Original magnification $\times 400$. * = $P < 0.0001$ versus healthy; # = $P < 0.0001$ versus all other markers within the SjS data series.